

# Systematic Elaboration of Trial Function Bases for the Study of Planar Structures

Isabelle Proust, Bruno Sauviac, Jean-Louis Amalric, and Henri Baudrand, *Senior Member, IEEE*

**Abstract**—This paper presents an integral method in combination with Green's functions and the boundary-element method to characterize a rectangular waveguide with electric or magnetic walls, loaded with a conductor of arbitrary cross section. The results provided by this method are in good agreement with available data in the literature. The modes of this type of waveguide are determined in the case of an arbitrarily shaped inner conductor with no consideration of size. The existence of the TEM mode has been verified. The modes calculated by this method are used as numerical basis functions in other applications. It is shown that they can be used to determine the resonant frequencies of a metallic patch or the input impedance of a planar antenna fed by a coaxial line. In this last case, the theoretical results are confronted with the experimental results.

**Index Terms**—Antenna theory, boundary-element method, coaxial waveguides, electromagnetic fields, Green's functions, integral equations, microstrip antennas, propagation.

## I. INTRODUCTION

THE cutoff wavenumbers or cutoff frequencies of a rectangular waveguide loaded with an inner conductor were calculated in many studies [1]–[3], by using different methods.

The method of partial regions [1] allowed the cutoff frequencies of a rectangular waveguide with corner ridges to be determined. Grüner [2] used the cutoff frequencies of a circular coaxial to determine the cutoff frequencies of a square coaxial having the same circumference. Swaminathan [4] located the cutoff wavenumbers of a waveguide with arbitrary cross section with the help of the current density on the inner conductor. However, the calculation of the current density becomes difficult when the inner conductor has small dimensions [5], which is why some authors use simplifying approximations [6]. Conciauro *et al.* [7] used the dyadic Green's function to calculate cutoff wavenumbers and modal fields in rectangular and circular waveguides, which are perturbed by cylindrical conductors.

In this paper, an integral method is used to characterize rectangular waveguides with electric or magnetic walls, loaded with a conductor of arbitrary cross section. The cutoff wavenumbers and the amplitude of longitudinal field components are determined with the use of Green's functions and the boundary-element method [8], [9]. The numerical problem can be easily implemented on personal computers.

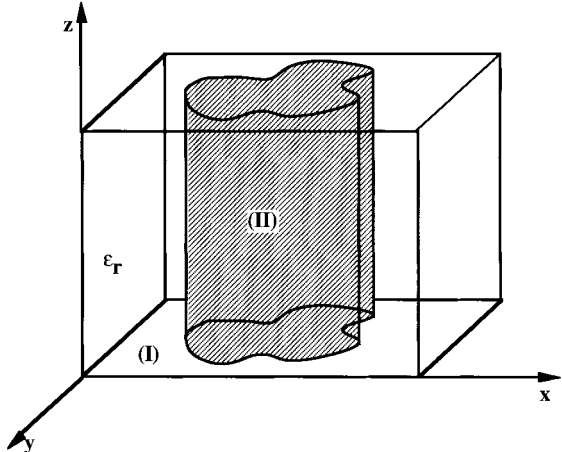


Fig. 1. General structure.

First, the theory is exposed. Obtained results are in good agreement with those available in the literature. The inner conductor is then either a cylinder with small radius or of triangular or hexagonal shape. In any case, the evaluation of longitudinal field components is presented.

The determination of cutoff wavenumbers and the longitudinal components  $E_z$  or  $H_z$  allows numerical basis functions that can be used to describe the electromagnetic fields in other applications to be created. Using these basis functions, we have calculated the resonant frequencies of a metallic patch and the input impedance of a planar antenna fed by a coaxial line.

## II. THEORY

The general structure analyzed is shown in Fig. 1. It is composed of a rectangular waveguide loaded with a conductor of arbitrary shape.

The rectangular shield can be either electric or magnetic. It is more interesting (with the purpose of studying planar antennas fed by a coaxial) to choose magnetic walls. Indeed, the magnetic walls could be placed closer to the structure than the electric walls [14]; this allows the convergence of the results to be obtained more rapidly.

Such a uniform waveguide generates TE and TM modes. The TEM mode exists as well, but this case will be treated separately.

The electromagnetic evolution in this type of waveguide is ruled by the Helmholtz's equation

$$(\nabla_t^2 + k_c^2) \begin{cases} E_z \\ H_z \end{cases} = 0 \quad (1)$$

Manuscript received July 19, 1994; revised June 20, 1997.

The authors are with the Laboratoire d'Electronique ENSEEIHT, 31071 Toulouse Cedex, France.

Publisher Item Identifier S 0018-9480(97)07100-7.

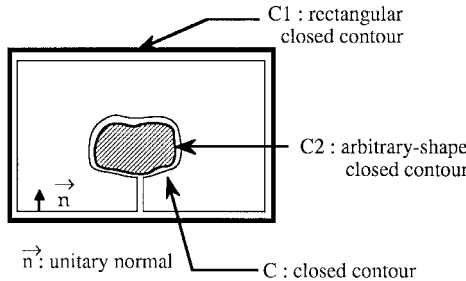


Fig. 2. Cross section of guide represented in Fig. 1.

where  $k_c$  is the cutoff wavenumber. The waves are supposed to propagate along the  $z$ -axis with the  $e^{-\gamma z}$  term, so

$$k_c^2 = \gamma^2 + k_o^2 \varepsilon_r$$

where  $\gamma$  is the propagation constant,  $k_o$  is the free-space wavenumber, and  $\varepsilon_r$  is the relative permittivity.

The problem is solved by using Green's functions. The equation to solve is given by

$$(\nabla_t^2 + k_c^2) G(M, M_o) = -\delta(M, M_o) \quad (2)$$

where  $G$  is the Green's function that verifies the same boundary conditions as the longitudinal field component  $E_z$  or  $H_z$ .  $M_o$  is the source point and  $M$  is the observation point.

These equations are associated with boundary conditions. In the case of an electric wall, the conditions are

$$E_z = 0$$

and

$$\frac{\partial H_z}{\partial n} = 0. \quad (3)$$

In the case of a magnetic wall (dual of electric wall), the conditions are

$$\frac{\partial E_z}{\partial n} = 0$$

and

$$H_z = 0. \quad (4)$$

The combination of (1) and (2) allows one to obtain the second Green's identity

$$\begin{aligned} \frac{E_z}{H_z} = & - \int_c G(M, M_o) \frac{\frac{\partial E_z}{\partial n_o}(M_o)}{\frac{\partial H_z}{\partial n_o}(M_o)} dl_o \\ & + \int_c \frac{\partial G}{\partial n_o}(M, M_o) \frac{E_z(M_o)}{H_z(M_o)} dl_o \end{aligned} \quad (5)$$

where  $c$  is a closed contour and  $\vec{n}$  is the normal vector, as indicated in Fig. 2.

The resolution of the problem then corresponds to solve the Green's second identity. The Green's function is chosen so that the boundary conditions (3) and (4) are automatically satisfied on the contour  $C1$ , which then allows simplification of the problem.

The expressions of the different Green's functions are the same as those given in [11]. To continue the resolution, TE and TM modes are considered separately and the boundary conditions are applied, as explained in [11]. Thus, the following equations are to be solved:

$$\text{TM modes} \quad \int_{C2} G(M, M_o) \frac{\partial E_z}{\partial n_o}(M_o) dl_o = 0 \quad (6)$$

$$\text{TE modes} \quad \int_{C2} \frac{\partial G}{\partial n_o}(M, M_o) H_z(M_o) dl_o - H_z(M_o) = 0. \quad (7)$$

The final equation to solve allows the electromagnetic evolution of the TEM mode to be determined.

The method previously described cannot be used because the longitudinal components of the TEM mode are equal to zero ( $E_z = H_z = 0$ ). Thus, the following Poisson's equation is used:

$$\nabla^2 \nabla = -\frac{\rho}{\varepsilon} \quad (8)$$

and by using the Green's functions [8]

$$V(M) = \int_{C2} \frac{\rho}{\varepsilon} G(M, M_o) dl_o \quad (9)$$

where  $\rho$  is the charge density,  $V$  is the potential applied on the inner conductor, and  $\varepsilon$  is the dielectric permittivity.

### III. NUMERICAL RESOLUTION

Equations (6), (7), and (9) are solved by the Galerkin's method and the application of the boundary-element method. The use of these methods leads to a homogeneous matrix system  $[A][x] = 0$  for (6) and (7) and to an inhomogeneous matrix system  $[A][x] = [B]$  for (9). The trial functions chosen are normalized step functions. Equations (6) and (7) can be written under the following form:

$$\text{TM modes} \quad \sum_{j=1}^N \frac{\partial E_z}{\partial n_j}(M_j) \iint_{\Gamma} \frac{G(M_i, M_j)}{\sqrt{d_i} \sqrt{d_j}} dl_i dl_j = 0 \quad (10)$$

$$\begin{aligned} \text{TE modes} \quad & \sum_{j=1}^N \frac{1}{2} H_z(M_j) + \sum_{j=1}^N H_z(M_j) \\ & \cdot \iint_{\Gamma} \frac{\frac{\partial G}{\partial n_j}(M_i, M_j)}{\sqrt{d_i} \sqrt{d_j}} dl_i dl_j = 0 \\ & \forall i \in \{1, \dots, N\} \end{aligned} \quad (11)$$

where  $N$  represents the number of segments on the contour  $C2$ , and  $d_i$  is the length of the  $i$ th segment.

The presence of the coefficient  $1/2$  in (11) is due to the fact that the Green's function is defined on a domain larger than that where the second Green's identity is applied. Theoretically, on the discontinuity contour  $C2$  (see Fig. 2) the Green's function varies abruptly from the value 1 in the dielectric to the value 0 in the metal. Whereas in practice, this function is continuous and presents oscillations on both sides

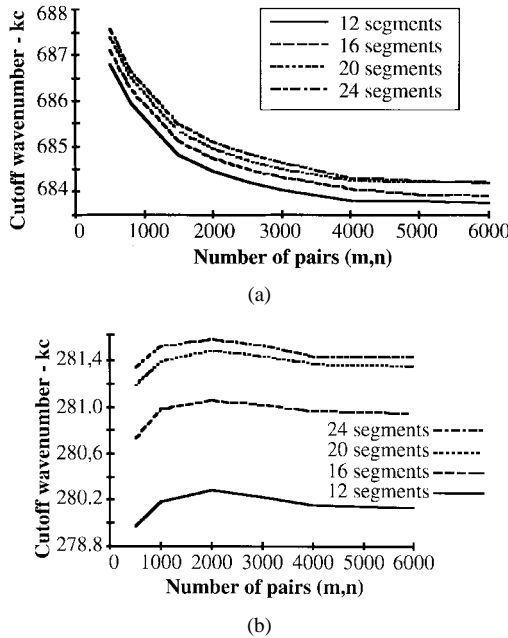


Fig. 3. (a) Convergence of the cutoff wavenumber of the first TM mode:  $c = 12.5$  mm,  $d = 10$  mm,  $a = 2.5$  mm,  $b = 4$  mm. (b) Convergence of the cutoff wavenumber of the second TE mode:  $c = 12.5$  mm,  $d = 10$  mm,  $a = 2.5$  mm,  $b = 4$  mm.

of the discontinuity (Gibbs' phenomenon). To approach the physical reality, the abrupt change of the function from 1 to 0 is avoided by considering that a middle state exists which takes the value of 1/2 [11].

In these systems, the unknowns are the cutoff wavenumbers  $k_c$  and the amplitudes of the  $\partial E_z / \partial n$  and  $H_z$  functions on each segment of the contour  $C2$ .

The following two methods of numerical resolution were tested.

1) *Direct Resolution*: The cutoff wavenumbers are determined by imposing that the determinant of the matrix of the homogeneous system should be zero. The rank of the system to be solved is  $N$ . The value of the cutoff wavenumber is then injected in the matrix. The resolution method consists of imposing the value to an unknown  $x_i$  (one of the  $N$  unknowns), to suppress the line  $i$  and the column  $i$ , and finally to solve along with the Cramer's Method the remaining inhomogeneous system that has a rank of  $N - 1$ .

2) *Resolution by the Least-Squares Method*: In this case, the homogeneous matrix system  $[A][X] = 0$  is solved by the least-squares method; it is the minimum of the functional  $X^t A^t A X$  that is searched for. This form is accompanied by the condition  $X^t X = 1$ . Thus, the following equality is obtained:

$$A^t A X = \lambda_{\min} X$$

where  $\lambda_{\min}$  is the minimum eigenvalue of  $A^t A$  and  $X$  is the eigenvector associated to this eigenvalue ( $t$  represents the transpose operation). A cutoff wavenumber sweep is applied to obtain the minimum eigenvalue. For each cutoff wavenumber, the minimum eigenvalue of the matrix  $A^t A$  is determined. Among these eigenvalues, we only keep the smallest. The corresponding cutoff wavenumber is the solution

TM MODES			
mode n°	SWAMINATHAN [4]	Our method	Relative error (%)
1	684.00	684.477	0.06
2	832.86	832.253	0.07
3	849.05	854.658	0.6
4	1029.59	1036.475	0.6
TE MODES			
mode n°	SWAMINATHAN [4]	Our method	Relative error (%)
1	207.89	203.949	1.9
2	284.65	281.39	1.1
3	396.31	396.107	0.05
4	528.64	513.082	2.9

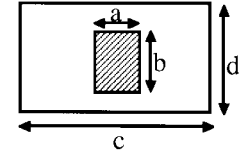


Fig. 4. Cutoff wavenumbers of a rectangular coaxial:  $c = 12.5$  mm,  $d = 10$  mm,  $a = 2.5$  mm,  $b = 4$  mm.

that is searched for. The corresponding eigenvector  $X$  could then be calculated.

The obtained results show that only the least-squares method gives systematically good results for the vector  $X$ . This vector (set of  $\partial E_z / \partial n$ ) or of  $H_z$ ) represents the unknown amplitudes of  $E_z$  or  $H_z$  on each segment of the discontinuity contour  $C2$ .

When the cutoff wavenumbers and the amplitudes of  $E_z$  or  $H_z$  on each segment of the contour  $C2$  are determined, the values of  $E_z$  and  $H_z$  can be obtained at each point of the structure. The transverse components are determined by application of Maxwell's equations. The three-dimensional (3-D) representation of  $E_z$  and  $H_z$  allows us to note that two properties are verified by showing that: 1) the field is equal to zero in the metallic part and 2) the boundary conditions on the discontinuity contour  $C2$  and on the external contour  $C1$  are well satisfied.

Now, let us examine the case of the TEM mode.

Equation (9) is written under the following form:

$$\text{TEM mode} \quad V_{oi} = \sum_{j=1}^N \frac{\rho_j}{\epsilon} \iint_{\Gamma} \frac{G(M_i, M_j)}{\sqrt{d_i} \sqrt{d_j}} dl_i dl_j \quad \forall i \in \{1, \dots, N\} \quad (12)$$

where  $V_o$  is the potential applied on the contour,  $\rho_j$  is the charge density,  $N$  is the number of segments on the contour  $C2$ , and  $d_i$  is the length of the  $i$ th segment.

In the case of the TEM mode, the unknowns are the values of  $\rho_j$  on each segment. When these data are calculated, the potential at each point of the structure is determined. The

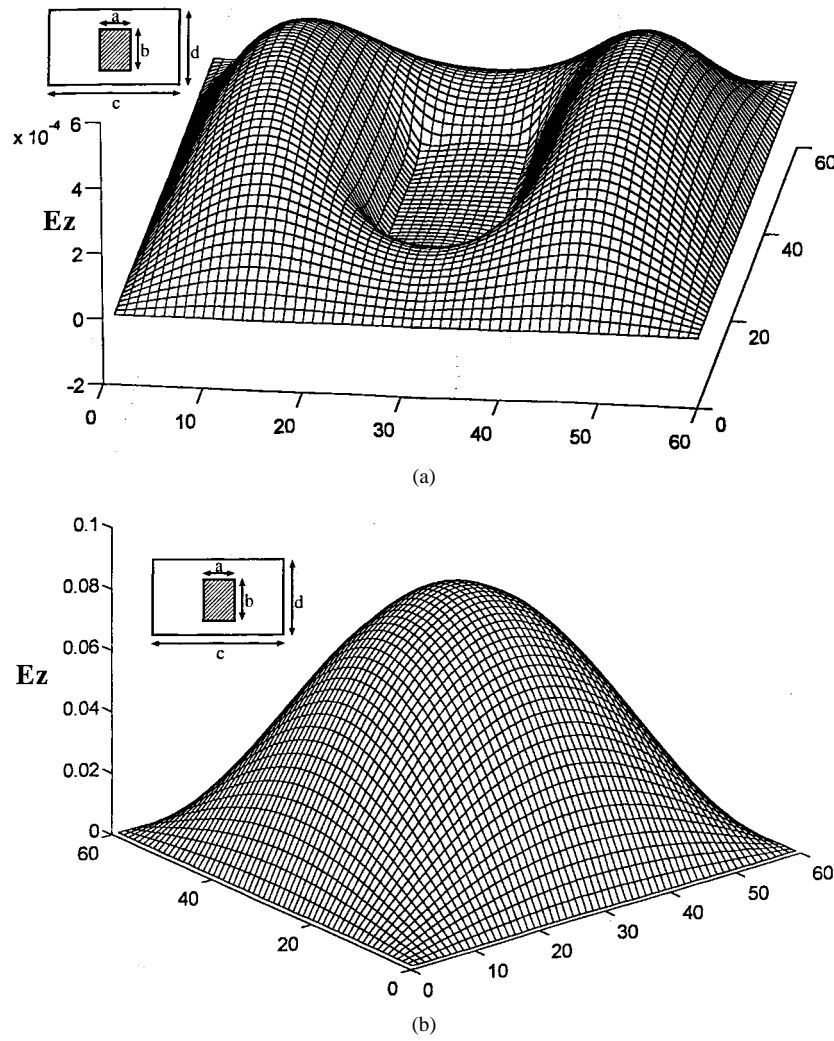


Fig. 5. (a) Longitudinal component  $E_z$  (vector  $\mathbf{X}$  calculated with the least-squares method):  $c = 12.5$  mm,  $d = 10$  mm,  $a = 2.5$  mm,  $b = 4$  mm. (b) Longitudinal component  $E_z$  (vector  $\mathbf{X}$  calculated with the Cramer's Method):  $c = 12.5$  mm,  $d = 10$  mm,  $a = 2.5$  mm,  $b = 4$  mm.

application of the relation  $\vec{E} = -\vec{\nabla}V$  allows us to obtain the electromagnetic field.

#### IV. RESULTS

##### A. Rectangular Coaxial

First, the convergence of the cutoff wavenumber as a function of the number of segments on the contour  $C2$  (see Fig. 2) and the number of pairs  $(m, n)$  in the series of the Green's function [11] is realized for two methods of resolution, with the results presented in Fig. 3(a) and (b). These studies were carried out for a rectangular coaxial waveguide whose dimensions are indicated in Fig. 3(a) and (b). Fig. 3(a) presents the convergence of the first TM mode and Fig. 3(b) the convergence of the second TE mode. The convergence studies are presented for only one method. It is obvious that the convergence of the cutoff wavenumber is obtained in the same way for the two methods—the matrix is the same for the two methods, but the numerical treatment is different. Fig. 3(a) and (b) allows us to observe that the convergence is obtained for 20 segments and 4000 pairs  $(m, n)$ .

In order to validate the method, the results are compared with those obtained by Swaminathan [4] in the case of a rectangular coaxial. Fig. 4 shows the good agreement between values of the cutoff wavenumbers of the first TE and TM modes determined by our method and by Swaminathan's approach. To determine the first cutoff wavenumber of the TE or TM modes, 10 s is sufficient by using a PC-486.

Fig. 5(a) and (b) shows the evolution of the  $E_z$  field for a given mode and Fig. 6(a) and (b) shows those of the  $H_z$  field. In Figs. 5(a) and 6(a) the vector  $\mathbf{X}$  was calculated with the least-squares method, while in Figs. 5(b) and 6(b) it was calculated with the help of the Cramer's Method. The initial imposed conditions are satisfied only if (10) and (11) are solved with the least-squares method. One of the steps of the "direct method" consists of solving a  $N$ -equations system with  $N$  unknowns. One of these unknowns is equal to 1, and if this unknown has a physical value close to zero, a considerable error occurs in the field calculation—which is why the obtained field could have no physical reality.

The method was also applied in the case of a magnetic shield. A representation of the fields  $E_z$  and  $H_z$  is given in Fig. 7(a) and (b).

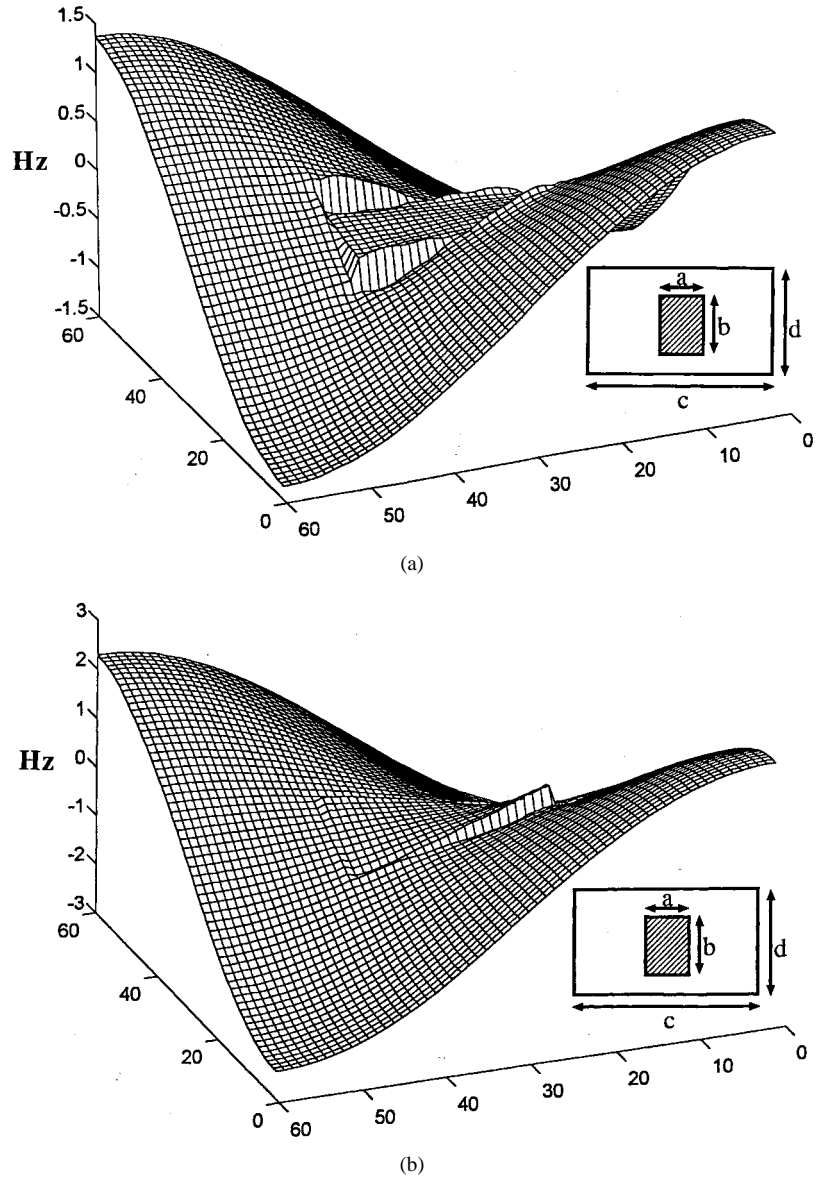


Fig. 6. (a) Longitudinal component  $H_z$  (vector  $\mathbf{X}$  calculated with the least-squares method):  $c = 12.5$  mm,  $d = 10$  mm,  $a = 2.5$  mm,  $b = 4$  mm. (b) Longitudinal component  $H_z$  (vector  $\mathbf{X}$  calculated with the Cramer's Method):  $c = 12.5$  mm,  $d = 10$  mm,  $a = 2.5$  mm,  $b = 4$  mm.

### B. Case of Small-Radius Cylindrical Conductor

When the contour  $C2$  is a circle of small radius, the results given by our method are compared with those obtained by a perturbation method [10]. These results are presented in Fig. 8. In this case (cylinder of small radius), two remarks could be added. Fig. 9(a) shows the evolution of the determinant of the matrix of the system in the case of the TE modes. The *poles* (values of  $k_c$  such that the denominator of the Green's function is equal to 0) and *zeros* (values of  $k_c$  such that the numerator of the Green's function is equal to 0) are very close, or are practically the same; the TE modes behave as if there were no metal in the structure, so they are not perturbed by the inner conductor. Fig. 9(b) shows the evolution of the determinant of the system matrix in the case of the TM modes. That is the first mode which is the more perturbed. The higher order modes are much less perturbed. These remarks confirm that the more the inner conductor is small, the more the structure looks like an empty waveguide.

### C. TEM Solution

If the shield of the waveguide represented in Fig. 1 is electrical, then the TEM mode exists because the structure is made up of two distinct conductors. Let us now consider a waveguide whose shield is magnetic. In this case, (12) also has a solution that looks like a TEM mode. This solution has no physical signification, but nevertheless, when the modes of the studied structure are used as basis functions, it is shown in [14] that this solution must be present in the modal decomposition.

Fig. 10(a)–(c) show the evolution, respectively, of the potential, the  $E_x$  and  $E_y$  components in the case of a rectangular inner conductor and electric shield.

### D. Structures of Original Shape

Developed software allows us to characterize structures in which the conductor has an arbitrary shape. Fig. 11(a)–(d) show the evolution of the  $E_z$  and  $H_z$  field in the case of

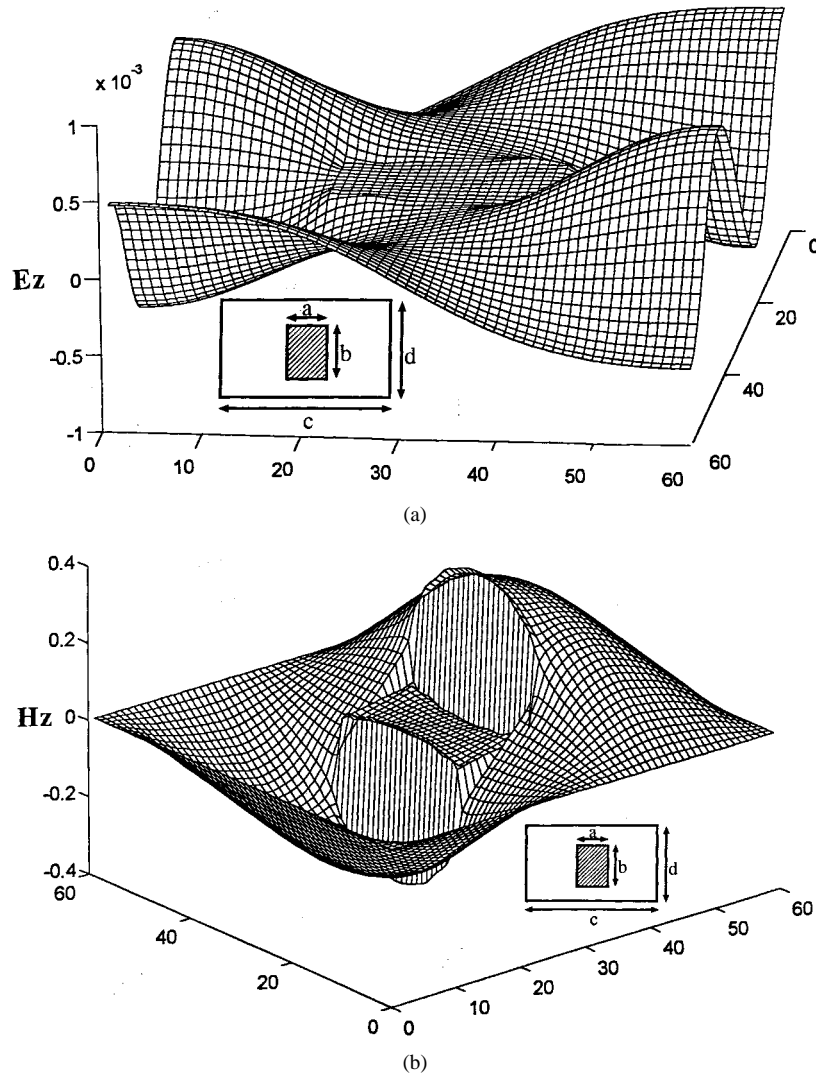


Fig. 7. (a) Longitudinal component  $E_z$  magnetic walls:  $c = 12.5$  mm,  $d = 10$  mm,  $a = 2.5$  mm,  $b = 4$  mm. (b) Longitudinal component  $H_z$  magnetic walls:  $c = 12.5$  mm,  $d = 10$  mm,  $a = 2.5$  mm,  $b = 4$  mm.

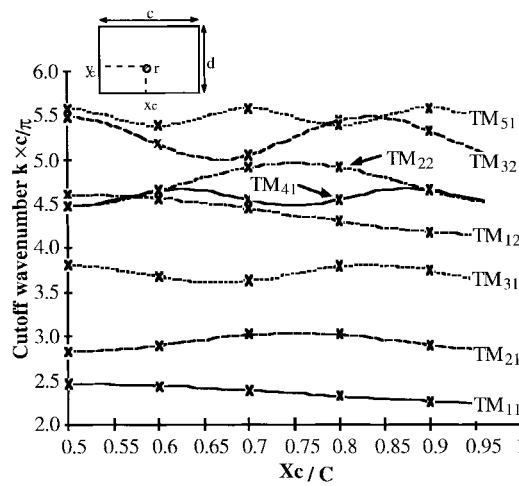


Fig. 8. Comparison between our method and the perturbation method:  $c = 90$  mm,  $d = 45$  mm,  $x_c = 45$  mm,  $y_c = 9$  mm,  $r = 2.7$  mm. Solid and dashed lines: our method, symbols: Davidovitch [10].

a triangular inner conductor for the electric shield [Fig. 11(a) and (b)] and magnetic shield [Fig. 11(c)–(d)].

## V. APPLICATIONS

### A. Calculation of the Resonance Frequency of a Patch

The studied structure is presented in Fig. 12(a). It is a dielectric substrate with one metallic face, and on the upper side, a metallic patch is placed. Here, the purpose will be to determine the resonant frequencies of this structure.

In order to do this calculation, the structure is placed in a rectangular box as indicated in Fig. 12(b). The structure is then composed of three parts: Part (I) is a rectangular empty waveguide with no top shield, Part (III) is a piece of rectangular waveguide filled with a dielectric, and Part (II) is the patch plane. The basis functions of the guides (I) and (III) are the modes of a rectangular waveguide. The test functions of Part (II) are determined numerically with the help of the previously exposed method. Indeed, the interface (II) is a cross section of the waveguide presented in Fig. 1.

The continuity relations of the tangential components of the electric and magnetic fields should be verified on each

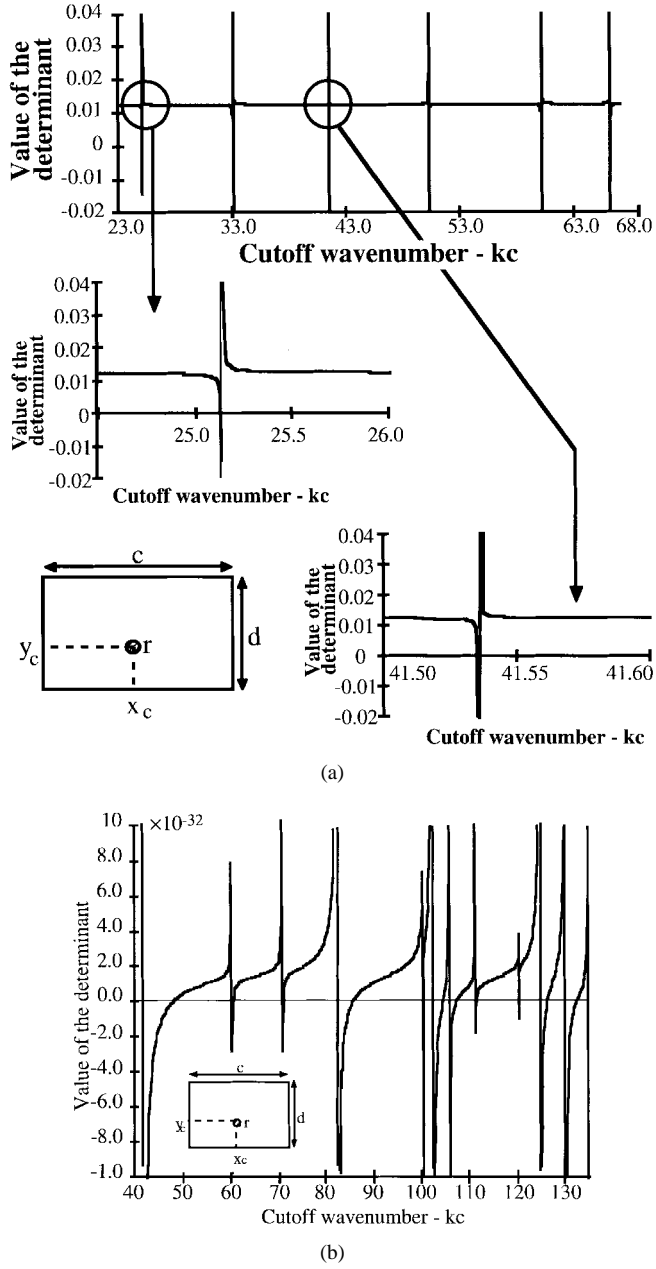


Fig. 9. (a) Evolution of the determinant TE modes small-radius cylinder conductor:  $c = 125$  mm,  $d = 95$  mm,  $x_c = 58$  mm,  $y_c = 44$  mm,  $r = 0.635$  mm. (b) Evolution of the determinant TM modes small-radius cylinder conductor:  $c = 125$  mm,  $d = 95$  mm,  $x_c = 58$  mm,  $y_c = 44$  mm,  $r = 0.635$  mm.

discontinuity [between Parts (I) and (II) and Parts (II) and (III)]. The parts of waveguides (I) and (III) are represented by operator admittance. The electric field in the plane (II) and the current densities on both sides of this plane are employed [13]. The use of the Galerkin's method leads to a homogeneous matrix system. The resonant frequencies are determined by imposing that the determinant of this matrix should be equal to zero. This method has been detailed in [13], [14].

The results obtained in this way are compared with the corresponding data in the literature [12]. Fig. 13(a) shows the good agreement between the values obtained with the help of the two methods. Fig. 13(b) shows the evolution of the determinant around the resonant frequency.

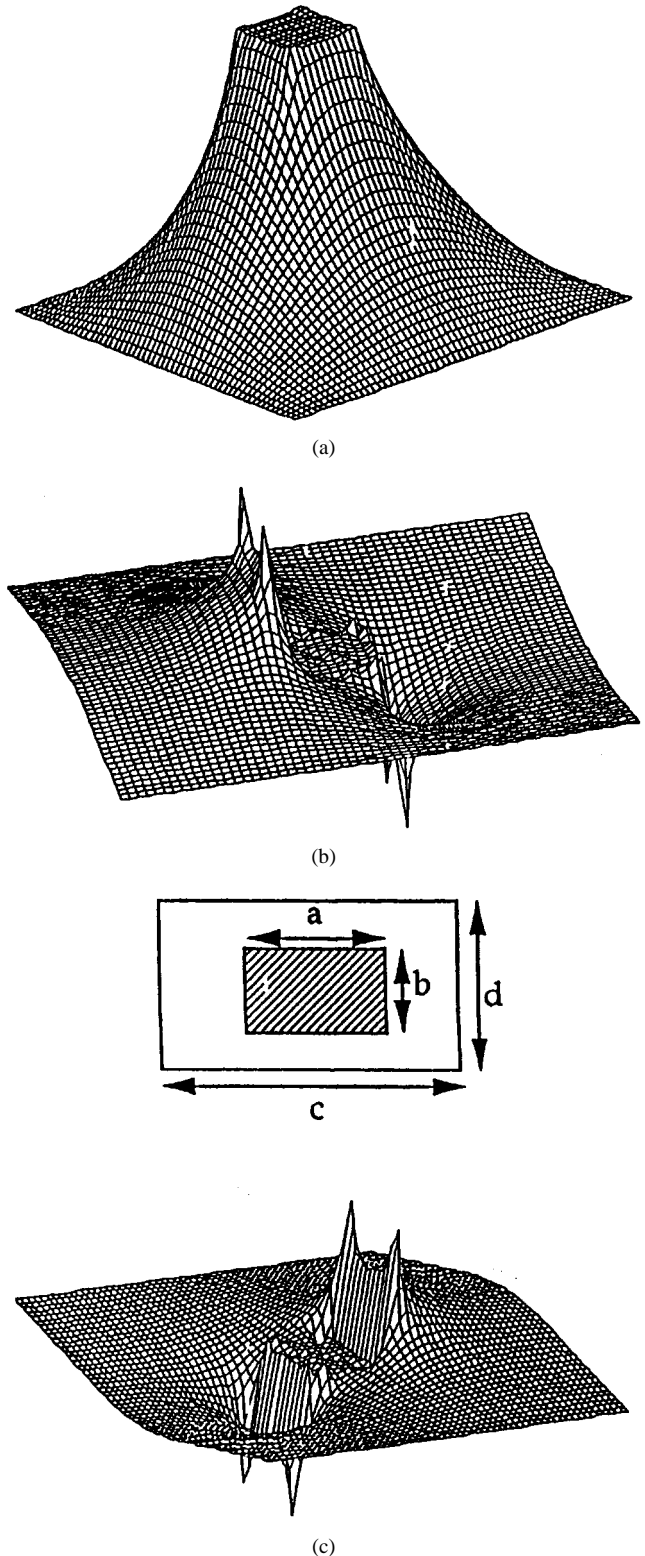


Fig. 10. (a) Potential: TEM mode. (b) Component  $E_x$ : TEM mode. (c) Component  $E_y$ : TEM mode,  $c = 125$  mm,  $d = 95$  mm,  $a = 25$  mm,  $b = 19$  mm,  $\epsilon_r = 2.2$  electric walls.

#### B. Input Impedance of a Planar Antenna Fed by a Coaxial Line

The studied structure is presented in Fig. 14. The metallic patch is placed on a dielectric slab and it is fed by a coaxial line.

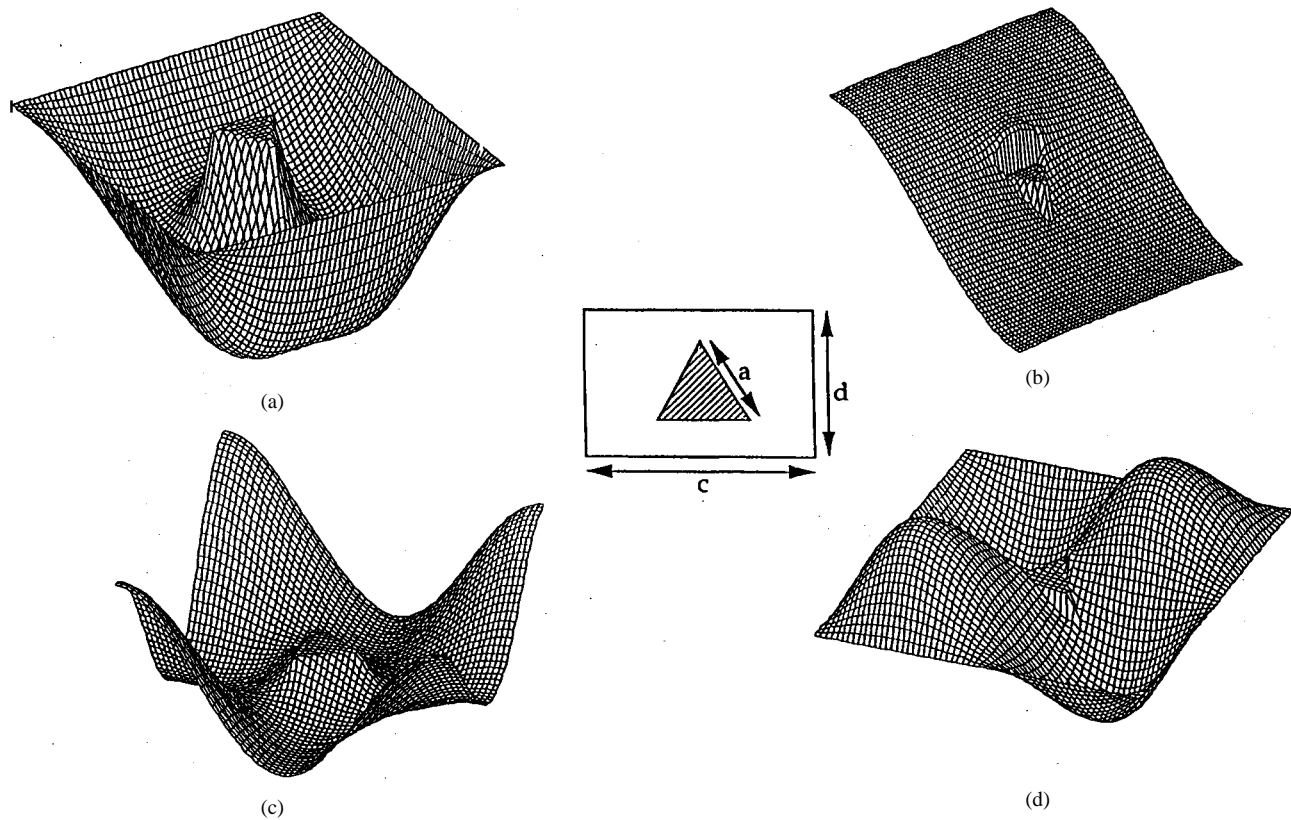


Fig. 11. (a)  $E_z$  component: electric walls. (b)  $H_z$  component: electric walls. (c)  $E_z$  component: magnetic walls, and (d)  $H_z$  component: magnetic walls,  $c = 300$  mm,  $d = 290$  mm,  $a = 60$  mm.

This paragraph shows that the method previously exposed allows us to determine the input impedance of the planar antenna.

As done above, the antenna is placed in a rectangular box (see Fig. 15). The structure is also composed of three parts. Parts (I) and (II) are the same as those described in the previous section. Part (III) is a rectangular guide of height  $h$  containing a dielectric and loaded by a metallic cylinder, similar to the waveguide represented in Fig. 1. The basis functions of this part of the guide are so determined.

As noted previously, the continuity relations of the tangential components of the electric and magnetic fields should be verified on each discontinuity. The magnitudes as admittance operator, current density, and electric field (chosen as trial function) are also used. In this case, the use of the Galerkin's method leads to a nonhomogeneous matrix system. The right-hand side (RHS) of this equation contains the influence of the antenna excitation. The input impedance is obtained using a variational form explicated in previous papers [13], [14].

Fig. 16 shows the input impedance of the structure. The patch antenna is rectangular and its dimensions are given in Fig. 16. Good agreement can be noted between our results and the measured data.

## VI. CONCLUSION

An integral method combined with Green's functions and the boundary-element method has been used to characterize

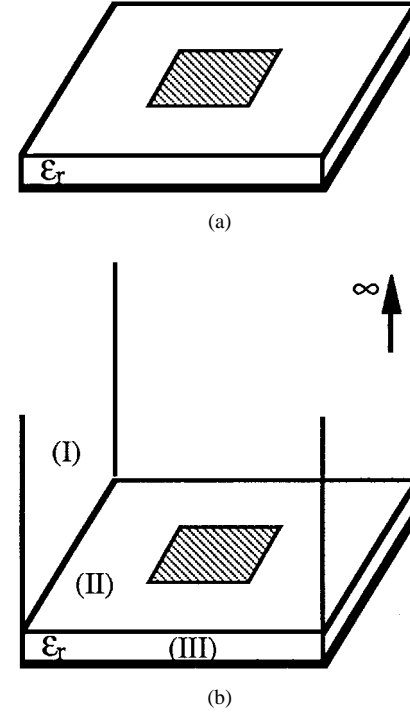


Fig. 12. (a) Patch deposited on a dielectric. (b) Patch deposited in a case.

the rectangular waveguides with an electric or magnetic shield loaded with an inner conductor of arbitrary shape.

	Our method	WENG CHO CHEW [12]	Measured
Resonance frequency (GHz)	11.96	11.94	12.04

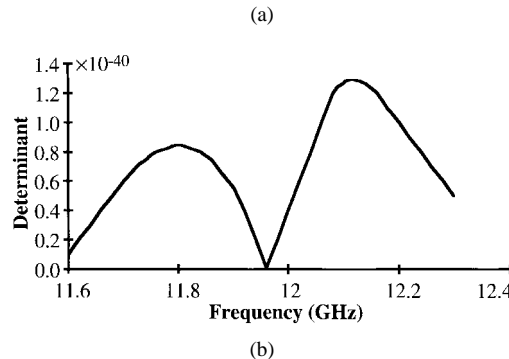


Fig. 13. (a) Resonance frequency of a rectangular microstrip patch. (b) Variation of the determinant around the resonance frequency.

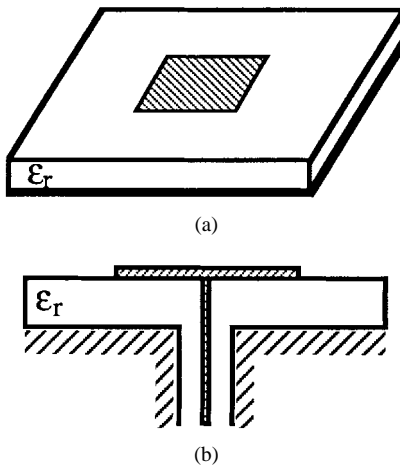


Fig. 14. Planar antenna loaded by a coaxial line. (a) Perspective view. (b) Cross view.

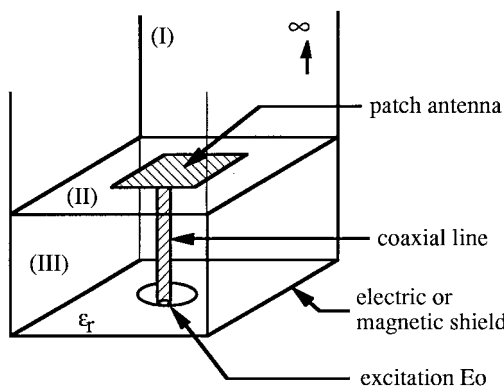


Fig. 15. Planar antenna deposited in a case.

The method has been validated by comparison between the results with those available in the literature in the case of a rectangular inner conductor. This method also allows the characterization of waveguides in which a conductor is of small dimensions.

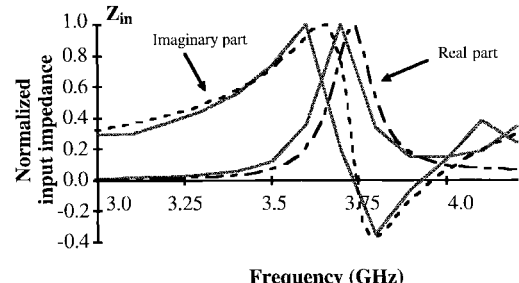


Fig. 16. Input impedance of a rectangular microstrip patch:  $c = 125$  mm,  $d = 95$  mm,  $a = 25$  mm,  $b = 19$  mm,  $h = 2.28$  mm,  $\epsilon_r = 2.2$ . Solid lines (computed results), dashed lines (measured results).

The determination of modes in such a structure allows us to generate a numerical basis of functions in which the electromagnetic field can be represented.

#### ACKNOWLEDGMENT

The authors wish to thank Prof. A. Papiernik, J. P. Damiano, and the Electronic Laboratory, University of Nice, Sophia-Antipolis, France, for their help and cooperation during the experimental measurements for this paper.

#### REFERENCES

- [1] L. Gruner "Characteristics of crossed rectangular coaxial structures," *IEEE Trans. Microwave Theory Tech.*, vol. MTT-28, pp. 622-627, June 1980.
- [2] ———, "Higher order modes in square coaxial lines," *IEEE Trans. Microwave Theory Tech.*, vol. MTT-31, pp. 770-771, Sept. 1983.
- [3] Q. C. Tham, "Modes and cutoff frequencies of crossed rectangular waveguides," *IEEE Trans. Microwave Theory Tech.*, vol. MTT-25, pp. 585-588, July 1977.
- [4] M. Swaminathan, E. Arvas, T. K. Sarkar, and A. R. Djordjevic, "Computation of cutoff wavenumbers of TE and TM modes in waveguides of arbitrary cross sections using a surface integral formulation," *IEEE Trans. Microwave Theory Tech.*, vol. 38, pp. 154-159, Feb. 1990.
- [5] J. P. Damiano and A. Papiernik, "Survey of analytical and numerical models for probe-fed microstrip antennas," *Proc. Inst. Elect. Eng. Microwave Antennas Propagat.*, vol. 141, no. 1, pp. 15-22, Feb. 1994.
- [6] F. Abboud, J. P. Damiano, and A. Papiernik, "Simple model for the input impedance of coax-fed rectangular microstrip patch antenna for CAD," *Proc. Inst. Elect. Eng.*, vol. 135, pt. H, no. 5, pp. 323-326, Oct. 1988.

- [7] G. Conciauro, M. Bressan, and C. Zuffada, "Waveguide modes via an integral equation leading to linear matrix eigenvalue problem," *IEEE Trans. Microwave Theory Tech.*, vol. MTT-32, pp. 1495–1504, Nov. 1984.
- [8] R. E. Collin, *Field Theory of Guided Waves*. Piscataway, NJ: IEEE Press, 1991.
- [9] C. A. Brebbia, *The Boundary Element Method for Engineers*. London, U.K.: Pentech, 1978.
- [10] M. Davidovitch and Y. T. Lo, "Cutoff wavenumbers and modes for annular-cross-section waveguide with eccentric inner conductor of small radius," *IEEE Trans. Microwave Theory Tech.*, vol. MTT-35, pp. 510–515, May 1987.
- [11] Z. Altman, D. Renaud, and H. Baudrand, "Integral equation scalar Green's function formulation for computation of cutoff wavenumbers and modal fields in waveguides," *IEEE Trans. Microwave Theory Tech.*, vol. 42, pp. 532–535, Mar. 1994.
- [12] W. C. Chew and Q. H. Liu, "Resonance frequency of a rectangular microstrip patch," *IEEE Trans. Antennas Propagat.*, vol. 36, pp. 1045–1055, Aug. 1988.
- [13] I. Proust, B. Sauviac, J. L. Amalric, and H. Baudrand, "Influence of feed probes on input impedance and performance of patch antennas," in *European Microwave Conf.*, Madrid, Spain, Sept. 1993, pp. 926–928.
- [14] I. Proust, "Contribution à l'étude des discontinuités en guides d'ondes coaxiaux. Application aux antennes planaires," Ph.D. dissertation, I.N.P. de Toulouse, France, 1994.



**Isabelle Proust** was born in Niort, France, in 1966. She received the Ph.D. degree in electronics from the Polytechnics National Institute of Toulouse, France, in 1994.

In 1995, she joined the French Atomic Energy Commission, CEA-CESTA, Le Barp, France, where she is studying antennas and substrate materials to improve performance of antennas. Her research has included modeling, manufacturing, and measuring planar antennas, and working on numerical methods.



**Bruno Sauviac** was born in Toulouse, France, on January 7, 1966. He received the Ph.D. degree in electronics from the Polytechnics National Institute of Toulouse, France, in 1993.

From 1987 to 1993, he was involved in the modeling of passive microwave circuits. He has also worked on inhomogeneous waveguides and cavities, waveguide discontinuity problems, dielectric resonators and patch antennas in the Electronics Laboratory of ENSEEIHT, Toulouse, France. From 1994 to 1996, he was at the French Atomic Energy Commission, CEA-CESTA, Le Barp, France. His research was on the modeling and the design of chiral media or bi-isotropic composites and, more generally, problems of heterogeneous media at microwave frequencies. In 1996, he joined the PIOM Laboratory, University of Bordeaux I, France, where he is studying electromagnetic interactions with chiral media, multilayered composites, and applications of chirality.

**Jean-Louis Amalric** was born in France in 1939. He received the Diplome d'Ingénieur degree in electronics and the Docteur-ès-Science degree in microwaves from the Institut National Polytechnique de Toulouse, France, in 1962 and 1978, respectively.

From 1970 to 1980, he worked on the realization and modeling of gyroelectric microwave circuit devices. He then worked on the modeling of passive microwave circuit and planar microantennas in the Microwaves Research Group of the Electronics Laboratory of ENSEEIHT, Toulouse, France, and is currently Professor of mathematics and microwaves and is in charge of the Education Department on Electronic and Signal Processing.

**Henri Baudrand** (M'86–SM'90) was born in France in 1939. He received the Diplome d'Ingénieur degree in electronics and the Docteur-ès-Science degree in microwaves, from the Institut National Polytechnique de Toulouse, France, in 1962 and 1966, respectively.

He is currently Professor of microwaves in charge of the Microwaves Research Group of the Electronics Laboratory of ENSEEIHT, Toulouse, France, where he works on the modeling of active and passive microwave circuit devices.